

## CALET measurements with cosmic nuclei and performance of the charge detectors

P. S. MARROCCHESI<sup>1</sup> FOR THE CALET COLLABORATION.

<sup>1</sup> Dept. of Physical Sciences, Earth and Environment, University of Siena, Via Roma 56, 53100 Siena (Italy)

marrocchesi@pi.infn.it

**Abstract:** CALET is an all-calorimetric electron telescope in preparation for a launch to the International Space Station (ISS), where it will be installed on the Exposure Facility of the Japanese Experiment Module (JEM-EF). With observations over a period of five years, CALET will be able to unveil the presence of possible nearby sources of high energy electrons and search for signatures of dark matter. The instrument includes a two-layered Charge Detector (CHD) module of scintillator paddles designed to identify - via a measurement of their electric charge - individual nuclear species from proton to iron and to detect trans-iron elements. Complementary charge information is provided by the Imaging Calorimeter (IMC).

CALET will be able to perform precision measurements of individual element spectra and of the energy dependence of secondary/primary abundance ratios. The extension of the present measurements of boron/carbon to the energy region above 1 TeV/amu will provide an important input to theoretical models of particle propagation in the galaxy.

In this paper, we will review the main physics goals of CALET measurements with nuclei, the expected performance of the charge detectors and the results of a prototype test with a fragmentation beam of relativistic ions that took place at the SPS of CERN in January 2013.

**Keywords:** secondary-to-primary ratios, charge identification

### 1 Introduction

CALET (CALorimetric Electron Telescope) is a Japanese led international mission funded by the Japanese Space Agency (JAXA), the Italian Space Agency (ASI), and NASA. The CALET instrument will be launched by a Japanese carrier and attached to the Exposure Facility (JEM-EF) on the International Space Station (ISS). The mission is expected to begin operations on the ISS in 2014 for a mission lifetime of 5 years.

The primary science goal of CALET is to perform high precision measurements of the electron spectrum from 1 GeV to 20 TeV. By integrating a sufficient exposure, CALET will be able to explore the energy region above 1 TeV, where the presence of nearby sources of acceleration is expected to shape the high end of the electron spectrum and leave faint, but detectable, footprints in the anisotropy. CALET will perform an accurate scan – with both electrons and gamma-rays – of the energy region already covered by previous experiments, taking advantage of a fine energy resolution and a low background contamination. The latter is made possible by the excellent proton rejection capability of the instrument that takes advantage of a full containment of the e.m. showers in the calorimeter and a detailed imaging of the first 3 radiation lengths. The precise measurement of the line shape of any spectral feature is expected to play a crucial role in the discrimination among different models of dark matter candidates, or it might suggest an alternative astrophysical interpretation. CALET will also monitor gamma ray transients with a dedicated Gamma-ray Burst Monitor (CGBM) and study solar modulation.

Equipped with a charge identifier module, placed at the top of the apparatus, and capable to identify the atomic number  $Z$  of the incoming cosmic ray, CALET will perform long exposure observations of cosmic nuclei from proton to iron and will detect trans-iron elements with a dynamic range up to  $Z=40$ . It will extend, by one order of magnitude in energy, the present measurements of the ratio of secondary to primary elements (e.g.: boron/carbon and sub-iron/iron), thereby providing information about the energy dependence of cosmic-ray propagation in the galaxy. In this paper, we focus on the detection of cosmic nuclei. Dedicated beam test measurements will be reported and the performance of the charge identification system of CALET will be discussed.

### 2 The CALET instrument

CALET is an all-calorimetric instrument, with a total thickness of 30 radiation lengths ( $X_0$ ) and 1.3 proton interaction lengths ( $\lambda_I$ ), preceded by a particle identification system. The energy measurement relies on two kinds of calorimeters: a fine grained pre-shower, known as imaging calorimeter (IMC), followed by a total absorption calorimeter (TASC). The effective geometrical factor of CALET for high energy electrons is  $\simeq 1,200 \text{ cm}^2 \text{ sr}$ . The total weight of the system will be approximately 650 kg. The schematic structure of the whole instrument with the main sub-detectors can be seen in Fig. 1. The Gamma-ray Burst Monitor is described elsewhere [1].

In order to identify individual chemical elements in the cosmic-ray flux, a Charge Detector (CHD) is positioned at the top of the CALET instrument to provide a measurement of the electric charge of the incoming particle via the

$Z^2$  dependence of the specific ionization loss in a double layered, segmented, plastic scintillator array. Each scintillator is 32mm wide, 448mm long and 10mm thick. The CHD and related front-end electronics are designed to provide incident particle identification over a large dynamic range for charges from  $Z=1$  to  $Z=40$  with sufficient charge resolution [2, 3] to resolve individual elements ( $\simeq 0.1e$  for light elements and  $\simeq 0.30 - 0.35e$  in the Fe region and above).

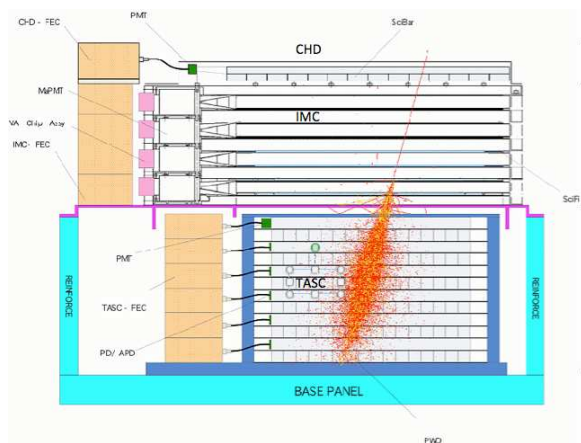


**Figure 1:** A schematic side view of the CALET instrument.

The IMC images the early shower profile with a fine granularity by using  $1 \text{ mm}^2$  scintillating fibers individually readout by multi-anode photomultipliers (MAPMT). It consists of 7 layers of tungsten plates, each separated by 2 layers of scintillating fibers (SciFi) with square cross section, arranged in belts along the x and y direction and is capped by an additional x,y SciFi layer pair. The transverse dimensions of the IMC are approximately 45 cm by 45 cm. The total thickness of the IMC is equivalent to  $3 X_0$ . The first 5 tungsten-SciFi layers sample the shower every  $0.2 X_0$  while the following 2 layers provide  $1.0 X_0$  sampling. The IMC is designed to: (i) separate the incident particles; (ii) determine the starting point of the shower; (iii) reconstruct the incident particle trajectory, and (iv) provide a coarse measurement of the particle's charge. The readout of the SciFi layers consists of multianode photomultiplier tubes with 64 anodes.

The TASC measures the total energy of the incident particle and discriminates electrons and gamma-rays from hadrons. The calorimeter is composed of 12 layers of Lead Tungstate (PWO) "logs", each with dimensions  $20\text{mm(H)} \times 19\text{mm(W)} \times 326\text{mm(L)}$ . The top PWO layer is readout by PMTs and a dual photodiode/avalanche-photodiode package (PD/APD) is used for the readout of the remaining layers (16 logs per layer). Alternate layers are oriented perpendicular to each other to provide x,y coordinates of the shower core. The total area of the TASC is about  $1,024 \text{ cm}^2$  and the total thickness is about  $27 X_0$  at normal incidence.

Charged particles and gamma rays  $> 10 \text{ GeV}$  will be triggered above a 15 MIP threshold from the sum of the last dynodes of the MAPMTs of the last layer of the IMC and a 55 MIP threshold from the sum of the PMTs of the first layer of the TASC. Electrons in the 1 GeV - 10 GeV range will be observed only for a limited exposure by reducing the IMC trigger threshold. The trigger rate above

10 GeV is estimated around 13 Hz.

### 3 Cosmic-ray spectral measurements

CALET [4] will identify cosmic-ray nuclei with individual element resolution and measure their energies in the range from a few tens of GeV to the PeV scale. It is expected that the CALET mission – after 5 years of operations on the ISS – will be able to extend to higher energies the present data on the elemental composition and energy spectra of charged cosmic rays from direct measurements. In particular, CALET should be able to extend the present balloon searches for a possible knee in the spectrum up to about 900 TeV for protons and up to 400 TeV/amu for He. Energy spectra of C, O, Ne, Mg, Si will be measured with sufficient statistical precision up to about 20 TeV/amu. Spectral features, like a hardening above 200 GeV/amu [5] or a deviation from a single power-law indicating the presence of a curvature in the spectrum, will be investigated.

### 4 Secondary-to-Primary Ratios

Direct measurements of the energy dependence of the flux ratio of secondary-to-primary elements – most notably boron/carbon – can discriminate among different propagation models. This observable is less prone to systematic errors than absolute flux measurements.

Above 10 GeV/amu, the dependence of the propagation path length is often parametrized in the form  $E^{-\delta}$ . An accurate measurement of the parameter  $\delta$  is crucial to derive the spectrum at the source by correcting the observed spectral shape for the energy dependence of the propagation term.

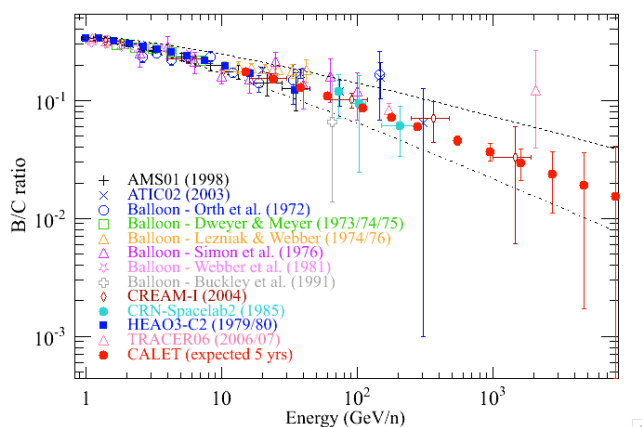


**Figure 2:** A partial compilation of the B/C ratio as a function of energy per nucleon and the expected statistical uncertainty after 5 years of observations with CALET.

These measurements have been pushed to the highest energies with Long Duration Balloon (LDB) experiments. However, at present, they remain statistics limited to a few hundred GeV/amu and suffer from a systematic uncertainty due to the residual atmospheric grammage at balloon altitude. The latter uncertainty becomes dominant in the TeV/amu region if  $\delta$  has a value close to 0.5, as the present data seem to suggest. Taking advantage of the long exposure in space and of the absence of atmosphere,

CALET can provide new data to improve the accuracy of the present measurements of the B/C ratio above 100 GeV/amu and extend them beyond 1 TeV/amu. A compilation of B/C data from direct measurements is shown in Fig. 2, where the data points expected from CALET in 5 years are marked as red filled circles in the energy range per nucleon from 15 GeV to 8 TeV.

## 5 Beam tests with relativistic ions

Measurements with prototypes of the CHD scintillators were performed in a dedicated beam test that took place at CERN in January 2013. Relativistic ions were extracted as secondary products from the interactions of a primary Pb beam of the SPS impinging on an internal Be target. Fully ionized nuclear fragments with  $A/Z=2$ , ranging from deuterium to heavy nuclei with atomic number  $Z>26$ , were steered along the H8 beam line of the SPS, where the CALET test apparatus was configured as summarized in the following. More than 15 million triggers were collected in two sets of runs with beam energies of 13 and 30 GeV/amu, respectively.

### 5.1 Layout of the CERN beam test

The CALET apparatus was preceded by a dedicated Beam Tracker that allowed for a precise reconstruction of the track and a very accurate identification of the charge of the incoming nucleus by means of 12 independent measurements of  $dE/dx$ . The Beam Tracker (Fig. 3) was subdivided into two sections: the Upper Tracker (UT) with 2 layers of Si strip detectors followed by 4 layers of Si pixel arrays, and the Bottom Tracker (BT) with 6 layers of Si strip detectors.

The Silicon pixel arrays – dedicated to the charge measurement – were comprised of  $500\mu\text{m}$  thick silicon sensors with 64 square pixels of  $1.28\text{ cm}^2$  sensitive area. The position measurement for the tracking was performed by silicon strip sensors, of the same thickness, with  $183\mu\text{m}$ -pitch strips that were ganged in parallel to obtain a total of 128 “strip-ribbons”, each  $732\mu\text{m}$  wide. The detectors were positioned with the strips perpendicular to the beam and alternately oriented in orthogonal directions. The Beam Tracker was designed and built in Italy.

It was followed by a CHD prototype module comprised of two X-Y layers, with a total of 6 scintillator paddles, covering an effective area of about  $100\text{ cm}^2$ . Each paddle consisted of a 10 mm thick scintillator, equipped with a light-guide and readout by an 8-dynode photomultiplier (Hamamatsu R11823).

### 5.2 Beam-tracker charge tagging

The trajectory of the incident beam particle was fitted, starting from the candidate points sampled along the track by the eight Si strip layers. The coordinates were reconstructed as the center of gravity of the cluster of hits formed by a “seed” strip (the one with the largest signal in the layer) and its two adjacent neighbours. Track quality was required by imposing a  $\chi^2$  cut.

The extrapolation of the track to the Si layers defined the impact points of the beam fragments with an rms position uncertainty of the order of  $20\mu\text{m}$  inside the UT, thus allowing to identify the pixel that had been hit by the incident track in each layer of the pixel arrays. The signals from the selected pixels were corrected for the path length

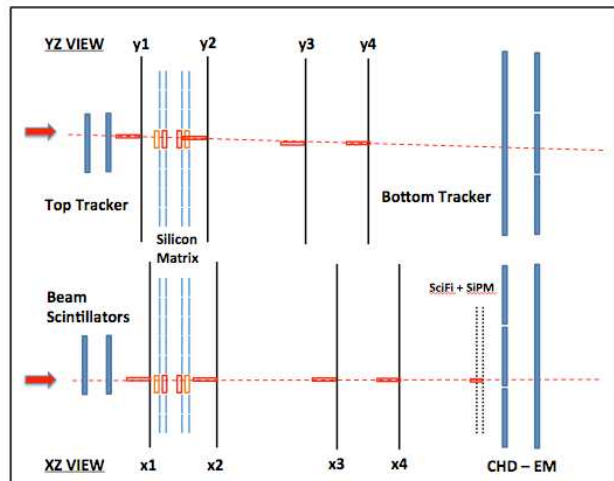


Figure 3: A schematic view of the beam tracker layout.

(estimated from the track parameters) traversed by the impinging particle in the silicon sensors.

Given the small total thickness of the tracker ( $< 0.3 X_0$ ), the amount of events where the incident particle interacted with its material was very limited. After equalization of the response of all channels (using muon data), the average value of 8 silicon strip layers and 4 silicon pixel layers is shown, as an example, in Fig. 4 for boron and carbon events. A charge resolution of  $0.1e$  was inferred from the fit of the two distributions. Further rejection was achieved in the data analysis using the correlation between the first and last pair of silicon strips layers, thus providing a high purity sample of non-interacting tracks.

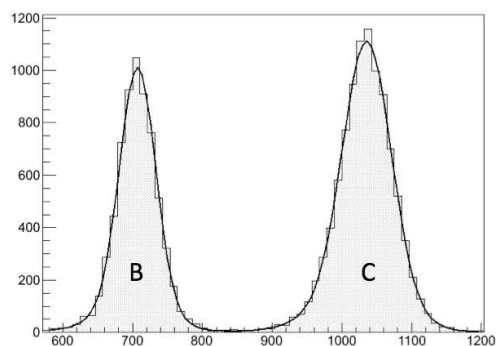
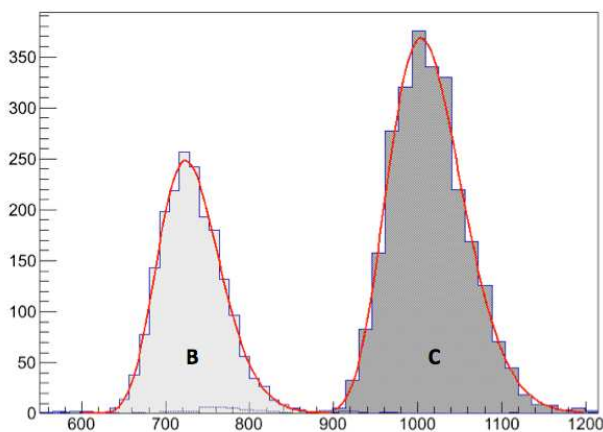


Figure 4: Charge tagging of B (left) and C (right) using multiple  $dE/dx$  measurements in the beam tracker (ADC units).

### 5.3 Performance of the CHD

The transverse position, with respect to the beam line, of each CHD scintillator was determined using the extrapolation of the track from the Beam Tracker to the CHD. Geometrical cuts were applied to define a fiducial region within the scintillator, free from edge and corner-clipping effects. The charge distribution from the combined measurements of the two CHD layers for a selected sample of boron and carbon nuclei is shown in Fig. 5.

A fit to both distributions provides an approximate estimator of the charge resolution in terms of the ratio  $\frac{\sigma}{\mu_{z+1} - \mu_z}$



**Figure 5:** Charge distributions for boron and carbon from the combined measurements of the two CHD layers (ADC units).

for two consecutive elements of atomic number  $Z$  and  $Z+1$ , with measured charges  $\mu_z$  and  $\mu_{z+1}$ , where  $\sigma$  is the average of the two uncertainties. Combining the information of the two CHD layers we get a charge resolution of  $\simeq 0.15e$  fulfilling the requirement for a  $5\sigma$  separation of boron from carbon. The contamination of the B sample due to charge-changing interactions of C (and heavier) nuclei in the CHD was carefully studied from the correlation plot of the upper vs lower CHD layers, using a high purity sample of carbon events. After removing uncorrelated events that were not compatible with the energy release for the same nucleus, the irreducible correlated background of C in the B sample was found not to exceed the 1.0 – 2.0% level, as expected from the simulations.

Another source of background that may affect B/C separation is backscattering from the calorimeter, an effect that is practically negligible at the beam test energy. It was studied with dedicated MC simulations at a flight energy of 1 TeV/amu, where it was found to contribute a fraction of misidentified boron events not larger than 1.2%.

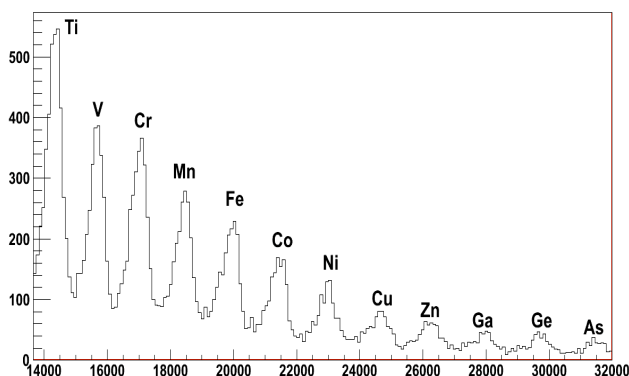


**Figure 6:** Selected sample of nuclei from Ti ( $Z=22$ ) to As ( $Z=33$ ) using the charge tagging provided by the Beam Tracker (ADC units).

Charge tagging with the Beam Tracker allowed the selection of a clean sample of heavier nuclei. As an example, the charge tagging performance for elements from Ti

( $Z=22$ ) to As ( $Z=33$ ) is shown in Fig. 6.

Using both layers of the CHD, individual elements could be identified as shown in Fig. 7, where Gaussian fits of the distributions indicate a charge resolution of the order of  $\simeq 0.30 - 0.35e$  in the region of iron, as obtained from a preliminary analysis of the 2013 beam test data, where the Fe signal is not yet corrected for the scintillator non linearity. The dynamic range of the CHD was shown to be adequate for the detection of even heavier nuclei (up to about  $Z=40$ ). However, the limited statistics collected at the beam test did not allow a sufficiently accurate determination of the charge resolution for  $Z > 33$ .

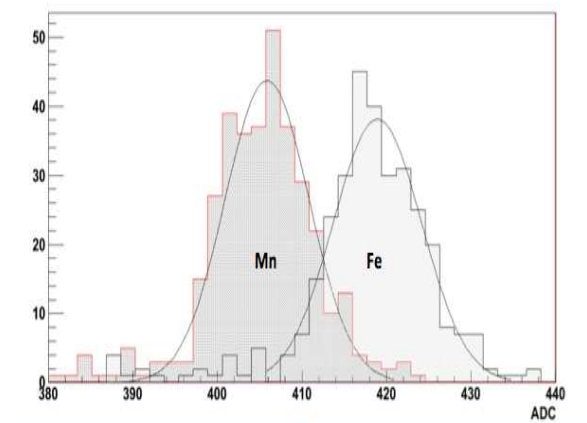


**Figure 7:** Charge distributions for Mn and Fe from the combined measurements of the two CHD layers (ADC units).

The non-linear response of the scintillator light yield as a function of  $Z^2$  was measured over the interval of elements spanning from  $^2H$  to Ni and was found to be in agreement with our previous measurements at a lower energy [3].

## 6 Conclusions

The 2013 beam test at CERN confirmed the results obtained in the previous beam tests at the Fragment Separator (FRS) of the GSI Helmholtzzentrum für Schwerionenforschung in Darmstadt [3] with a lower energy (1.3 GeV/amu) and at HIMAC in Japan [2]. Preliminary results from the measurements of relativistic fully ionized nuclear fragments ranging from  $1 \leq Z \leq 33$ , confirmed an expected charge resolution close to  $0.15e$  for light nuclei, like B and C, while reaching an almost constant value of  $0.30 - 0.35e$  in the region of iron.

The measurements of the even lighter elements, like  $^2H$  and He, and the analysis of the complementary charge information from the IMC fibers will be reported in a separate publication.

## References

- [1] K. Yamaoka et al.: Proc. of the 32nd Int. Cosmic Ray Conference (2011)
- [2] Y. Shimizu et al.: Proc. of the 32nd Int. Cosmic Ray Conference (2011)
- [3] P.S.Marrocchesi et al.: Nucl. Instrum. Meth. A 659 477 (2011)
- [4] S. Torii et al.: Nucl. Instrum. Meth. A630 55 (2011)
- [5] H. S. Ahn et al: Astrophys.J. 714 L89-L93 (2010)